AGU PUBLICATIONS

Geophysical Research Letters

RESEARCH LETTER
10.1002/2017GL073245

Key Points:
- We combine airborne gravity with other data to provide a more definite view of the bed topography of a major outlet glacier in Greenland
- Based on the refined bed topography, we project that Jakobshavn Isbræ will keep retreating into deeper grounds for decades to come
- High-resolution gravity data helps fill gaps in major outlet glacier bed mapping where traditional deep radar sounding methods fail

Supporting Information:
- Supporting Information S1

Correspondence to:
L. An,
an.lu@uci.edu

Citation:
An, L., E. Rignot, S. Elieff, M. Morlighem, R. Millan, J. Mouginot, D. M. Holland, D. Holland, and J. Paden (2017), Bed elevation of Jakobshavn Isbræ, West Greenland, from high-resolution airborne gravity and other data, *Geophys. Res. Lett.*, *44*, 3728–3736, doi:10.1002/2017GL073245.

Received 27 FEB 2017
Accepted 29 MAR 2017
Accepted article online 3 APR 2017
Published online 30 APR 2017

Bed elevation of Jakobshavn Isbræ, West Greenland, from high-resolution airborne gravity and other data

L. An[1], E. Rignot[1,2], S. Elieff[3], M. Morlighem[1], R. Millan[1], J. Mouginot[1], D. M. Holland[4], D. Holland[4], and J. Paden[5]

[1]Department Earth System Science, University of California, Irvine, California, USA, [2]Jet Propulsion Laboratory, California Institute of Technology, Pasadena, California, USA, [3]Sander Geophysics, Ottawa, Ontario, Canada, [4]Courant Institute of Mathematical Sciences, New York University, New York, New York, USA, [5]CReSIS Center, University of Kansas, Lawrence, Kansas, USA

Abstract Jakobshavn Isbræ, West Greenland, which holds a 0.6 m sea level volume equivalent, has been speeding up and retreating since the late 1990s. Interpretation of its retreat has been hindered by difficulties in measuring its ice thickness with airborne radar depth sounders. Here we employ high-resolution, helicopter-borne gravity data from 2012 to reconstruct its bed elevation within 50 km of the ocean margin using a three-dimensional inversion constrained by fjord bathymetry data offshore and a mass conservation algorithm inland. We find the glacier trough to be asymmetric and several 100 m deeper than estimated previously in the lower part. From 1996 to 2016, the grounding line migrated at 0.6 km/yr from 700 m to 1100 m depth. Upstream, the bed drops to 1600 m over 10 km then slowly climbs to 1200 m depth in 40 km. Jakobshavn Isbræ will continue to retreat along a retrograde slope for decades to come.

1. Introduction

The contribution to sea level rise from the Greenland Ice Sheet has increased significantly in the past decades due to the accelerated flow of its glaciers and the enhanced melting of its snow and ice surface [e.g., *Rignot et al.*, 2011a]. Jakobshavn Isbræ (JI), in West Greenland, is the largest and most active outlet glacier. It drains 6.5% of the ice sheet area [*Echelmeyer et al.*, 1991]. Repeated laser altimeter surveys by NASA's Airborne Topographic Mapper (ATM) showed that the glacier experienced a slight thickening between 1991 and 1997 of 10 cm/yr [*Thomas et al.*, 1995] while many other glaciers were thinning. After 1997, the glacier started to thin [*Thomas et al.*, 2003] and accelerate [*Joughin et al.*, 2004; *Luckman and Murray*, 2005]. The glacier floating ice tongue collapsed in 2002–2003 [*Weidick et al.*, 2004] after experiencing thinning rates of up to 80 m/yr [*Thomas et al.*, 2003]. The ice shelf removal reduced the back stress on the glacier, causing its ice speed to triple [*Joughin et al.*, 2008]. As the glacier retreated, the frontal regions thinned up to 15 m/yr [*Thomas et al.*, 2009].

This drastic evolution following decades of slow retreat since the little ice age has been attributed to the intrusion of warmer-than-usual, salty, subsurface (below 400 m depth) Atlantic waters (AW) into Ilulissat fjord in the mid-1990s [*Holland et al.*, 2008]. The higher heat content of the fjord waters fueled higher rates of ice shelf melt causing it to collapse. *Motyka et al.* [2011] estimated from mass conservation that the ice shelf melted at 228 ± 49 m/yr in the 1980s. The melt rate must have therefore increased by 35% in the late 1990s to explain the observed 80 m/yr thinning. As a result of the ice shelf collapse and glacier acceleration, JI contributed a 1 mm global sea level rise from 2000 to 2011 [*Howat et al.*, 2011].

To interpret the glacier evolution and reduce uncertainties in projections of its evolution, it is essential to know the glacier thickness, bed elevation below sea level (bsl), and fjord bathymetry. The slope in bed topography exerts a major control on the rate of grounding line retreat [*Schoof*, 2007]. The retreat is expected to be rapid along retrograde portions of the bed, i.e., where the bed elevation slopes in the inland direction, because a higher ice thickness entrains higher spreading rates. Conversely, bumps in bed topography will slow down the retreat due to a reduction in spreading rate. This instability is referred to as the marine ice sheet instability or tide-water glacier cycle [*Post et al.*, 2011]. In the fjord, bathymetry controls the advection of warm, salty AW toward the grounding line. Deep portions of the fjord facilitate the intrusion of subsurface AW, whereas shallow parts (<300 m) restrict its access to the glacier [*Holland et al.*, 2008].

To this day, the fjord bathymetry and glacier bed topography of the lower portion of JI have remained poorly known, at least not sufficiently well to provide reliable information for ice sheet numerical models. Standard vessels cannot penetrate the fjord to measure its depth due to the permanent presence of icebergs, brash ice, and ice mélange caused by a 350 m deep sill at the mouth of the fjord which blocks the exit of icebergs. On land, the sounding of bed topography in the lower reaches of the glacier using the Multichannel Coherent Radar Depth Sounder (MCoRDS) is rendered difficult by the thick ice (2 km), the presence of highly absorptive and temperate ice near the bottom, combined with high surface clutter caused by a broken up ice surface [*Leuschen et al.*, 2010]. Seismic profiles were successfully collected upstream of the terminus by *Clarke and Echelmeyer* [1996]. Together with quality radar data upstream, these observations revealed the presence of a deep trough beneath JI, more than 1 km bsl, extending far inland [e.g., *Plummer et al.*, 2008]. Near the ice front, few reliable bed echoes are available. Radar sounders do not provide a comprehensive description of the bed topography, hence leaving considerable uncertainty about the depth of JI close to the ocean margin.

Here we use airborne gravity data collected in August 2012 on board a Eurocopter AS-355 F2 helicopter using the Sander Geophysics Ltd (SGL) AIRGrav system [*Argyle et al.*, 2000]. The AIRGrav system achieves unprecedented spatial resolution (750 m) and precision (0.5 mGal) in gravity mapping. We combine the gravity data with novel, discrete measurements of the fjord bathymetry and a revised reconstruction of bed topography using a mass conservation (MC) approach [*Morlighem et al.*, 2014]. We apply a three-dimensional inversion of the gravity data between the fjord data and the MC reconstruction to infer the bed topography in between. We discuss the results, their accuracy, and their impacts on interpreting glacier changes and projecting them for decades to come.

2. Data and Methods

We conducted a helicopter-borne, high-resolution (750 m) gravimetric survey of several glaciers including JI using SGL's AIRGrav system over a period of 2 weeks. AIRGrav is an inertially referenced gravimeter that uses a Schuler-tuned inertial platform [*Cochran and Bell*, 2010]. AIRGrav has three orthogonal accelerometers and two 2 degrees-of-freedom gyroscopes mounted on its inertial platform [*Argyle et al.*, 2000]. The primary gravity sensor is the vertical accelerometer, which is held within 10 arc sec (0.0028°) to the local vertical. With suitable postprocessing, the accelerometers and gyroscopes are sufficient to determine the vector gravity components to the sub-mGal level (1 mGal = 10^{-5} m^2/s). AIRGrav is capable of drape flying over terrain, i.e., provide reliable estimates of the free air gravity anomalies even when the system does not fly at a constant elevation [*Argyle et al.*, 2000; *Studinger et al.*, 2008]. The final resolution and accuracy of the AIRGrav data depend on the survey design. Slower aircraft speed and tighter flight line spacing improve the resolution and accuracy. Typical surveys deliver data with noise levels better than 0.5 mGal with a half sine wave ground resolution ranging from a few hundred meters to a few kilometers depending on the survey speed. A Novatel OEM4 and OEMV GPS receivers, and data loggers provide average position of the helicopter and raw range information at 10 Hz. The comparative navigation data supplied during production flights allows for differently postprocessed GPS corrections for every survey flight. The helicopter also carried a Riegl LD90-31K-HiP Infrared Laser Rangefinder with a range of 1500 m, a resolution of 1 cm, an accuracy of 5 cm, and a data rate of 3.3 Hz. SGL proprietary geophysical software was used for AIRGrav data processing. As the Gordon and Betty Moore Foundation (GBMF) funded the survey, we refer to the free-air gravity anomaly data as the GBMF gravity data in this paper.

We surveyed a 500 m spacing grid, at an average ground speed of 56 knots (29 m/s), with a ground clearance of 80 m (Figure 1). NASA Operation IceBridge (OIB) surveyed JI with AIRGrav from year 2010 to year 2012 at a ground speed of 262 knots (135 m/s) with a 500 m clearance. The slower flight speed and tighter spacing of the GBMF data yield a data grid with a spatial resolution of 750 m versus 4700 m along-track for the OIB data filtered with a 35 s half-wavelength time filter. The spatial resolution of the GBMF data is therefore 6 times better than OIB. We evaluate the measurement error of the 750 m gridded data at 0.5 mGal based on an analysis of crossover errors.

We use the GBMF data to simulate the impact of a change in aircraft speed and ground clearance on the spatial resolution, noise level, and magnitude of the gravity anomalies recorded over the JI trough. Height changes are simulated by upward continuing the GBMF data to a new height of the aircraft (Figure S1 in the supporting information). Speed changes are simulated by increasing the duration of the time filter applied on the GBMF data. Faster speeds and higher ground clearances reduce the spatial resolution and the amplitude

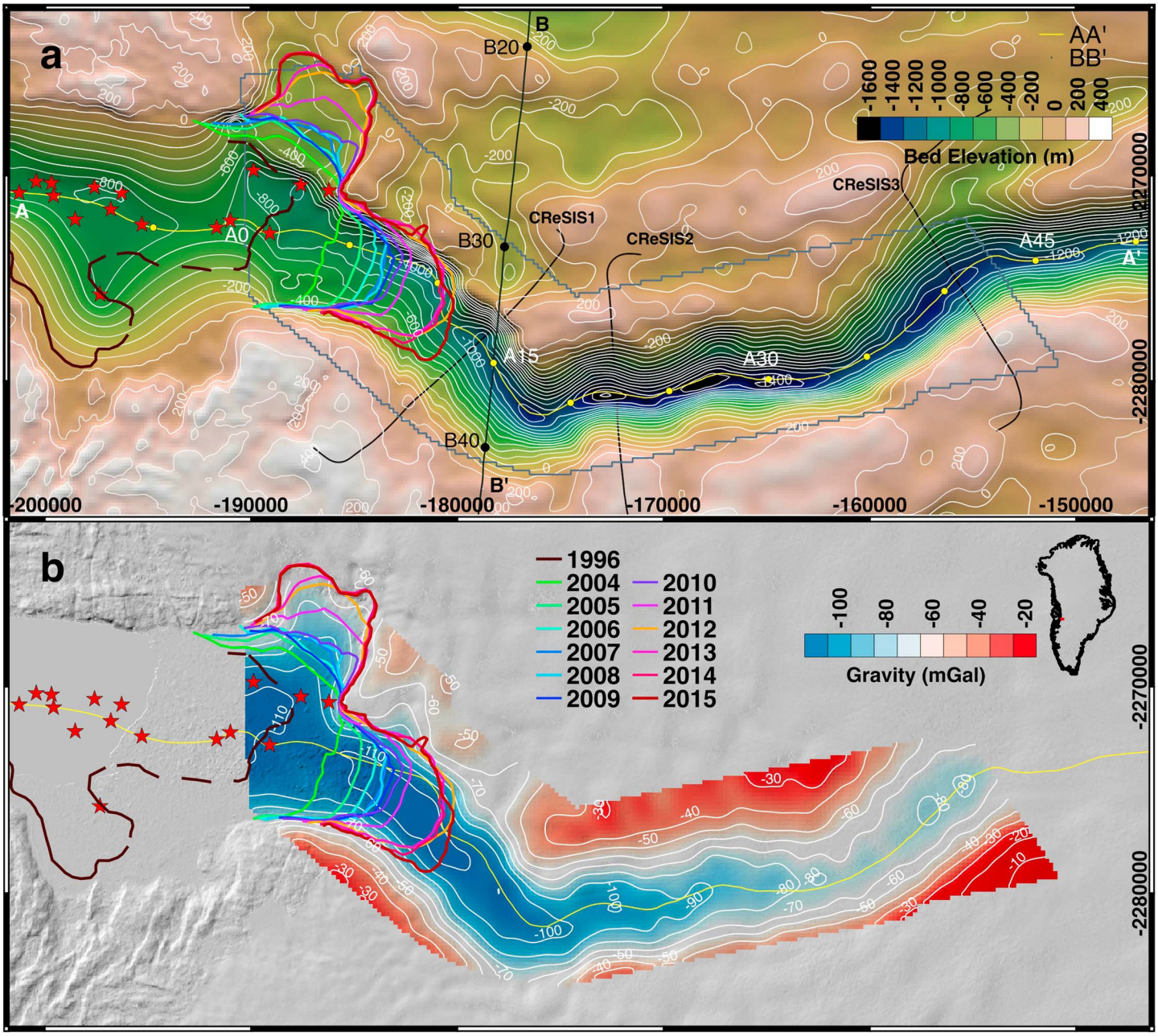

Figure 1. (a) Bed elevation above mean sea level of Jakobshavn Isbræ (JI), West Greenland, and fjord bathymetry reconstructed from a 3-D inversion of the GBMF gravity data, color coded from white to brown (400 m to 0 m above sea level) to green, blue, and dark blue (200 to 1600 m below sea level) with 100 m contours in white. Profile A-A′ with yellow dots every 5 km is shown in Figure 3, profile B-B′ in Figures S1–S2 in the supporting information, and profiles CReSIS1-3 in Figure 2. The limit of the survey domain is a thin, dark blue outline. Grounding line positions are color coded from brown (1996 from ERS-1/2) to green, blue, and red (2004 to 2015 from Landsat). Discrete depth soundings in the fjord are red stars. Background is a shaded relief digital elevation model of Greenland [*Howat et al.*, 2014]. Projection is polar stereographic north at 150 m spacing. (b) Airborne, high-resolution, free-air gravity anomalies from the year 2012 GBMF survey with a color scale in mGal (1 mGal = 10^{-5} m^2/s) and 10 mGal contours in white. Survey lines are thin black lines. Inset on top right shows glacier location in Greenland.

of the gravity anomalies recorded over the trough. We also evaluate the impact of applying different filter lengths on data resolution and data noise (Figure S2).

Bathymetry was measured from eXpendable Current profiler (XCP) and Conductivity Temperature Depth (XCTD) probes dropped from helicopters between 2009 and 2015. A total of four points lay within the GBMF survey (Figure 1). Additional soundings from the remainder of the fjord are integrated in the final product. To interpolate the fjord data, we use a water depth of zero along the fjord margins, a Delaunay triangulation

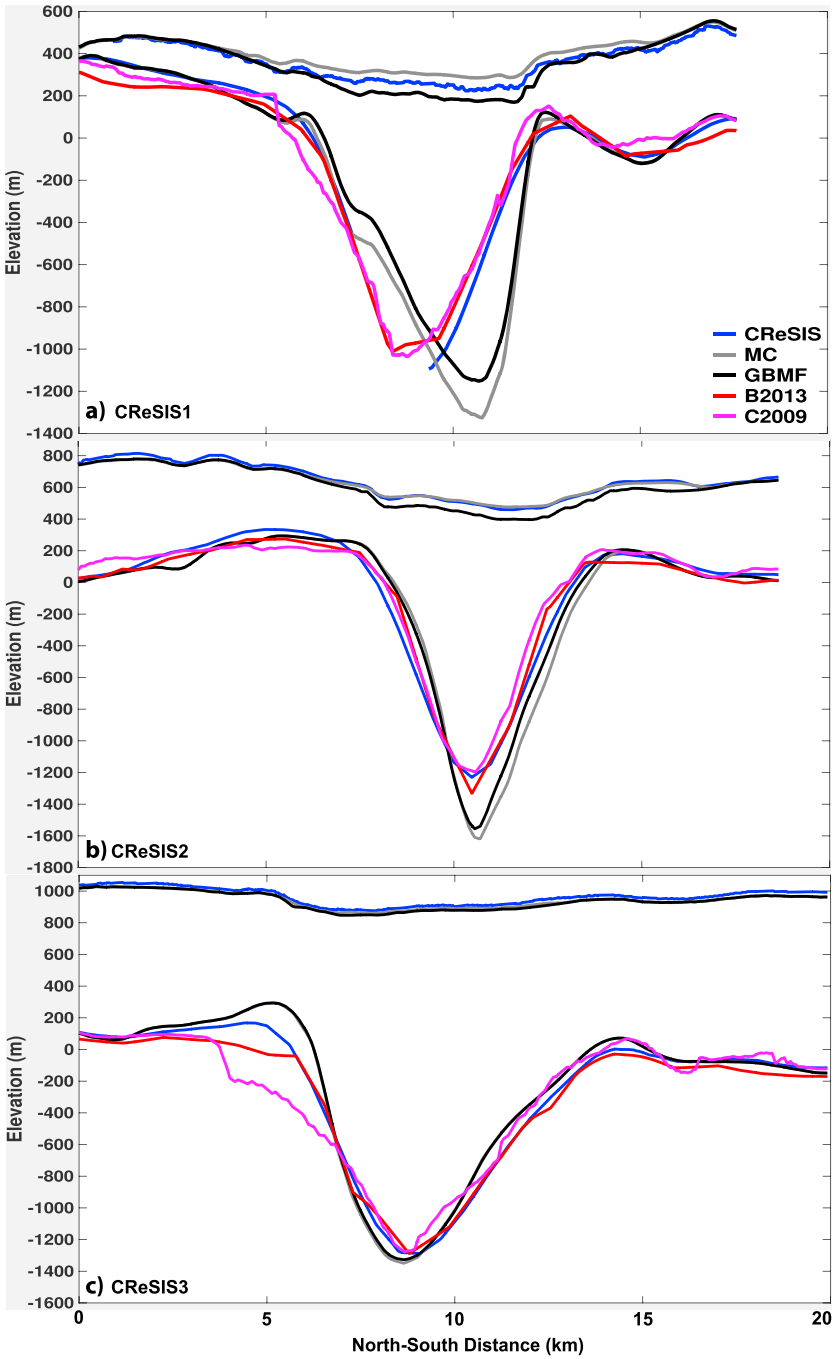

Figure 2. Comparison of the bed elevation Jakobshavn Isbræ, West Greenland, from the MC reconstruction (grey), the GBMF gravity survey (black), *Bamber et al.* [2013] (red) and *Joughin et al.* [2014] (purple) along profiles (a) CReSIS1, (b) CReSIS2, and (c) CReSIS3 in Figure 1, at low, medium, and high elevation along the trough, respectively, along with surface elevation from CReSIS (blue) in 2009, GBMF in 2012 (black), and MC/B2013/C2009 in 2007–2008 (grey). Direction is north to south from left to right.

between discrete depth recordings at the fjord center, and additional constraints from the MC reconstruction at the ice-ocean boundary.

To analyze the gravity data, we employ the Geosoft GM-SYS 3-D software, which implements *Parker*, 's [1973] method. The inversion domain is modeled as three layers: (1) a solid ice layer with a density of 0.917 g/cm^3; (2) a sea water layer with a density of 1.028 g/cm^3; and (3) a rock/sediment substrate layer with a uniform density of 2.72 g/cm^3. Selection of a density for rock is discussed later on. Ice surface elevation is from the

GBMF laser altimeter. The model domain extends to the limit of the GBMF survey. Beyond the survey domain, we use the initial bed model to calculate the gravity field using a forward model based on GM-SYS 3-D (Figure S3). The initial bed model is the interpolated bathymetry for the fjord and the MC result on land. We match the observed gravity and forward modeled gravity at the boundary by estimating the DC shift to apply on the data in the upper part of the survey domain where the MC result is most reliable because quality ice thickness data exist. We allow a 1.5 km wide transition at the ocean boundary and at the boundary with the modeled gravity. Within the transition boundary, the inversion is modulated by a factor varying linearly between 0 (no gravity inversion) to 1 (full gravity inversion) as a function of distance to the gravity survey. No data inversion is performed outside the domain (inversion factor is 0). During the inversion, the unknown bed elevation is modified iteratively until we obtain the best match between modeled and observed gravity. The iteration stops when the calculated gravity does not vary by more than 0.1 mGal.

To define an optimal average density for the glacier bed, we calculate the rate of convergence of the solution in terms of the misfit between modeled and initial gravity fields for densities varying from 2.6 to 3.0 g/cm^3 with steps of 0.05 g/cm^3. We find a minimum at a density of 2.72 g/cm^3 (Figure S4). A value of 2.72 g/cm^3 is consistent with the presence of orthogneiss, mainly granodioritic to tonalitic, in the area [*Pedersen et al.*, 2013].

We use the gravity misfit, i.e., modeled gravity minus observed gravity, to quantify the uncertainty of the inversion (Figure S5). The inversion significantly reduces the gravity misfit from the initial bed, as expected. To translate the misfit (in mGal) into an error in bed elevation, we calculate the gravity anomaly using GM-SYS 3-D obtained by shifting the bed result by +100 m and compare the results with the original gravity field. We find an average shift of 5 mGal in gravity per 100 m of ice in the trough. We use this product to generate a point-per-point conversion of the gravity misfit into an uncertainty in bed elevation (Figure S6). Given that the gravity misfit ranges from −3 to +3 mGal, the nominal precision of our bed mapping is about 60 m.

Existing radar-derived thickness data from MCoRDS were used to produce an updated MC result for the bed, ice thickness, and error (Figure S6). The MC result is gridded at 150 m spacing, with a spatial resolution of 350 m. The MC map is better in terms of resolution and accuracy than *Bamber et al.*'s [2013] 1 km spacing map, or B2013, which uses kriging on land and the International Bathymetric Chart of the Arctic Ocean (IBCAO) v3 in the fjord [*Jakobsson et al.*, 2012]. We also compare the GBMF result with the bed map of *Joughin et al.* [2014], generated by CReSIS in 2009 and which we refer to as C2009.

We map the grounding line of JI using ERS-1/2 interferometric SAR data from year 1996, ERS-1 orbits 22386 and 22887 and ERS-2 orbits 2713 and 3214, frames 1890, following *Rignot et al.* [2011b]. While interferometric fringes are not visible across the entire grounding line, especially the northern tributary, the results capture the 1996 position over the deepest part of the glacier and on its near-stagnant ice shelf (Figure S7). We complement this information with the mapping of ice rumples by *Clarke and Echelmeyer* [1996] to get a near-continuous mapping.

Following the ice shelf collapse in 2002–2003, *Rosenau et al.* [2013] showed that the glacier developed a floating section only about 100 m long along the ice front; i.e., the grounding line has remained within 100 m of the calving front after 2003. Combining the 1996 interferometric data with ice front positions recorded from Landsat data in late summer conditions (late August to early September), we obtain a 20 year proxy record for the grounding line retreat of JI (Figures 1 and 3).

3. Results

GBMF gravity data with 20, 28, 36, and 42 s half-wavelength filters provide similar gravity anomalies over the JI trough, except for a reduction in data noise for the longer filters (Figure S2). This similarity indicates that the GBMF data fully resolves the gravity anomaly associated with the JI trough. The gravity anomaly along profile B-B′ decreases rapidly when the aircraft speed exceeds 70 m/s (Figure S1). At 140 m/s, the gravity anomaly is reduced by 10 mGal, which would translate into an error in bed elevation of 200 m. With the OIB data, which include both higher speed (140 m/s) and higher ground clearance (450 m), the gravity anomaly is 25 mGal too low above the JI trough; i.e., the data would yield a bed elevation 500 m too high. Changing the ground clearance has a stronger impact on data quality than changing the speed (Figure S1). Upward continuing the data to the OIB height reduces the gravity anomaly by 23 mGal, equivalent to 460 m of ice. Upward continuing the data to 250 m height reduces the gravity anomaly by only 8 mGal or 160 m of ice equivalent. We conclude

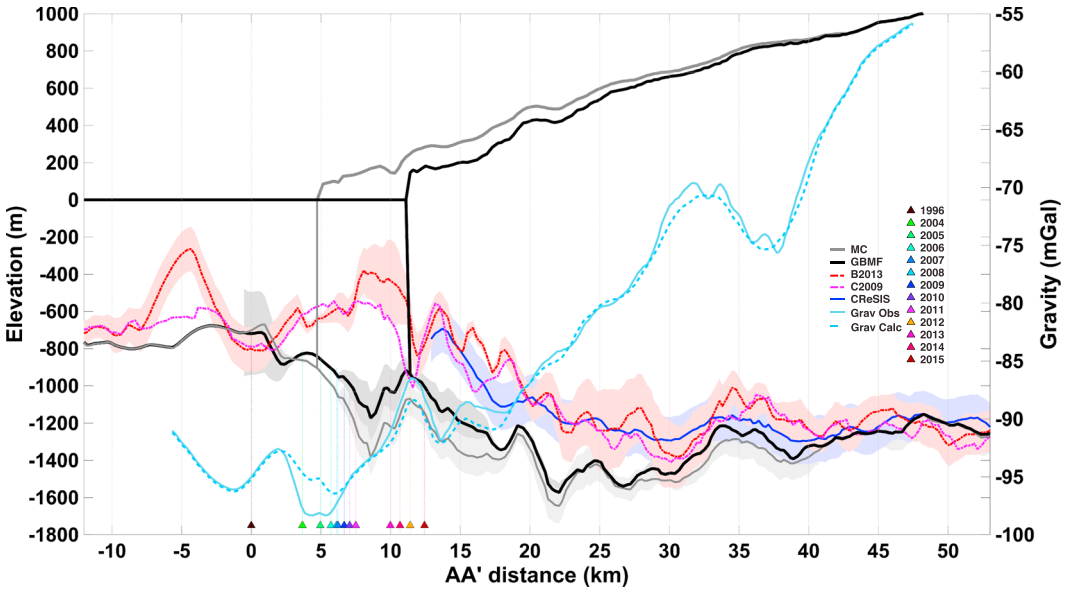

Figure 3. Profile A-A′ along the deepest bed of Jakobshavn Isbræ, West Greenland, showing the surface and bed elevations from the MC reconstruction (grey), the GBMF data in this study (black), *Bamber et al.* [2013] (dotted red), *Joughin et al.* [2014] (dotted purple), and CReSIS (dark blue) with corresponding error bars in shaded color (±1 *sigma*). The surface elevation is from year 2007 to 2008 (MC, B2013,C2009) and 2012 (GBMF). Red stars denote bathymetry data in the fjord. Colored triangles denote the positions of the glacier grounding lines at different epochs with the same color table as in Figure 1. Origin of distance is the 1996 grounding line position. Superimposed on that plot with a secondary vertical axis on the left-hand side is a comparison of the observed gravity anomaly (continuous blue) versus the calculated (dotted blue) gravity anomaly in mGal along profile A-A′.

that while there is flexibility in aircraft speed below 70 m/s, it is critical to maintain a ground clearance <200 m to detect the gravity anomaly over JI trough within less than 5 mGal.

Our model does not use a layer of sediment. A simple Bouguer slab calculation shows that each 100 m of sediment with density 2.2 g/cm^3 leads to a bed elevation overestimate by 30 m. To explain the gravity anomaly measured by OIB over the JI trough, one would need a 1500 m thick layer of sediments to match existing ice thickness measurements. We conclude that the OIB data cannot be used to detect the depth of the JI trough. The only gravity data that are sensitive enough to detect the deepest bed are from the GBMF survey.

The observed gravity anomalies vary from −20 mGal to −120 mGal, with peak values along the trough and near the grounding zone (Figure 1b). Bed elevation is well correlated with the gravity anomaly (Figure 1a), except in the last 15 km where the bed map is asymmetric: the bed is steeper and deeper on the north-side, and smoother and shallower on the southside. The northern branch of the glacier terminates abruptly in the ocean. The asymmetry is present in seismic profile S8 of *Clarke and Echelmeyer* [1996] approximately located at km 16. Upstream of km 20, the bed is symmetric, with a bed depth of 1600 m at km 22 from the 1996 grounding line (Figure 3). Bumps and hollows in inferred bed elevation greater than 60 m are above the noise level.

Rosenau et al. [2013] reported a 3.5 ± 0.2 km grounding line retreat for 2004–2010, or 0.6 km/yr, similar to the value from *Joughin et al.* [2012] for 2006–2009. Here we estimate 0.62 km/yr for the entire period 1996 to 2016, with a total grounding line retreat of 12.5 km at the glacier center. During that time period, the ice shelf front retreated by 18 km.

The inversion yields a smooth transition in bed topography between the GBMF data and the MC result but at a lower spatial resolution. Following the line of deepest bed, we find that the bed depth drops from 700 m at the center of the grounding line in 1996 to 1100 m bsl at the 2015 grounding line. Farther upstream, the bed depth drops to 1600 m at km 22, then slowly rises to 1200 m over the next 40 km. From km 0 to 27, the bed is essentially retrograde, consistent with earlier studies but several 100 m deeper [*Joughin et al.*, 2012; *Gogineni et al.*, 2014]. The grounding line retreated rapidly from 2011 to 2012, before retreating more slowly as the glacier encountered a shallower bed.

A comparison of GBMF with MC shows that GBMF is about 100 m deeper in the lower reaches (Figure 2a and Figure 3, km 5 to 20) i.e., 5%, but within error bars. Farther upstream, the two solutions are in good agreement (Figures 2b and 2c). Comparing the errors from GBMF and MC (Figure S6), the MC result has an uncertainty of 100 m over most of the trough, whereas GBMF has an error varying from 30 m to 140 m. Farther upstream, the errors in MC and GBMF are more similar.

B2013 has a sill depth of 200 m (km 5) in the fjord that is an artifact and a bump at 400 m depth (km 8 to 11) that is also an artifact. The B2013 bed depth is 600 m too shallow compared to GBMF or 60% at km 10. The difference remains above noise level until km 30. The two solutions do not converge until km 45. The bumps along A-A′ from km 5 to 30 are not confirmed by the GBMF or MC. We attribute these artifacts to krigging of sparse radar data; a more detailed discussion of these could be found in the supporting information (Figures S8 and S9) [*Bamber et al.*, 2013; *Joughin et al.*, 2014].

Comparing the GBMF results with MCoRDS, we find a reasonable agreement above km 33 (Figure 2c), but errors as large as 500 m at km 14 (Figures S8 and S9). We attribute this discrepancy to the difficulty of identifying bed echoes near the ocean margin [*Gogineni et al.*, 2014]. We also compare the results with C2009 along the profile from *Joughin et al.* [2014] (Figure S10) and along the line of deepest bed (Figure 3). We find significant differences of 200–300 m and a poor correlation in bed variability below km 30.

4. Discussion

Our inversion does not include a sediment layer. Inversions for basal shear stress [*Joughin et al.*, 2014; *Sergienko et al.*, 2014; *Shapero et al.*, 2016] suggest the presence of a weak bed, possibly a few meters to 100 m thick. In our inversion, introducing a layer of 100 m thick sediments would change the bed elevation by only 30 m. This magnitude uncertainty is less than the uncertainty of our gravity inversion. The GBMF result also agrees with MC in the upper part of the survey domain where quality thickness data exist, which suggests that the presence of sediments is not necessary to explain the gravity data.

Our study demonstrates the practical use of high-resolution airborne gravity to fill critical gaps in bed elevation in Greenland, especially in deep fjords that cannot be surveyed with deep radar sounders. If available, radar echo sounding would be preferable since these data are more precise (10–30 m versus 60 m) and higher resolution (10 m versus 750 m). Where reliable thickness data exist, the MC solution provides a high-resolution solution with low errors. Closer to the ocean margin where radar echoes are challenging to interpret, the gravity data offer a seamless mapping. To obtain a spatial resolution comparable to MC, the helicopter would need to fly at least twice slower, with a line spacing about twice denser, which would quadruple the cost of the survey.

Our results have implications for interpreting the retreat of JI since 1996. First, they suggest that the grounding line may have been anchored on a 700 m sill in the 1990s, before retreating into a fjord about 400 m deeper. Following the rapid retreat until 2012, the glacier has reached a higher bed which slowed down the retreat temporarily, as projected by *Joughin et al.* [2012] despite uncertainties in prior bed mappings. Second, during the retreat, as noted by *Joughin et al.* [2012], the glacier calving front has remained within 20 m of hydrostatic equilibrium. Ice front thickness will therefore increase from a current 1100 m at km 12.5 (bed at 1000 m depth) to 1700 m when the glacier grounding line will reach at km 22 (bed about 1500 m depth) or 50%, which will increase the ice discharge accordingly. Third, the results confirm that there is not a major bed obstacle that could slow down the retreat at least until km 30. Fourth, the grounding line is currently 400 m deeper than estimated previously; hence, thermal forcing from the ocean is 0.4°C greater from the pressure dependence of the freezing point of seawater alone.

At a fixed position along the glacier main trunk, the annual average ice velocity has been increasing steadily over time [e.g., *Joughin et al.*, 2014]. At the center of the calving front, however, we find that the mean annual speed averaged 12.6 $\pm$ 0.9 km/yr from 2002 to 2015 (Table S1); i.e., the annual calving speed, which is the sum of the ice front speed and the retreat rate, has been about 13.2 $\pm$ 0.9 km/yr, with little to no long-term trend, hence equivalent to a maximum rate of calving.

The new bed elevation confirms earlier studies [e.g., *Thomas*, 2004; *Joughin et al.*, 2012] that JI is undergoing a marine ice sheet instability, since it is retreating along mostly a retrograde bed. The retreat was likely triggered by an increase in ice shelf melt rate due to the intrusion of warmer AW in the fjord [*Holland et al.*, 2008]. The current retreat rate of 0.6 km/yr is half as large as that observed in West Antarctica for Pine Island and Thwaites

glaciers(1 km/yr) and one third as large as that experienced by Smith Glacier (2 km/yr) [*Rignot et al.*, 2014]. These values place upper bounds on the current rate of retreat of large glaciers undergoing marine instability. JI is probably retreating slower, because it is confined in a deep trough with narrow sides that provide strong lateral resistance to flow.

The GBMF bed data provide a significantly improved description of bed topography in the lower reaches of the glacier, in reasonable agreement with the MC reconstruction. This new topography will be of interest to modeling studies used to project or reconstruct the glacier evolution and the ocean circulation in the fjord. A similar approach should be used in fjords often choked up with iceberg debris, e.g., Helheim or Kangerdlugssuaq glaciers, and with poor radio echo sounding data near the calving fronts.

5. Conclusions

We employ high-resolution airborne gravity acquired at a low aircraft speed, with low ground clearance, to resolve the bed topography — and ice thickness — of Jakobshavn Isbræ, west Greenland, in three dimensions using observational constraints offshore (bathymetry) and onshore (MC solution). The results provide a more definite view of the bed topography of this major glacier system than available previously, however, at a spatial resolution of 750 m along the trough and with an average precision of about 60 m. The results reveal an asymmetric bed in the lower reaches of the glacier, with a deeper bed along the northern flank of the trough, and a bed 300–400 m deeper on average than estimated previously, yet consistent with the presence of a retrograde bed favorable to fast retreat. The bed configuration upstream of the current grounding line suggests that the glacier will continue retreating for many decades to come.

Acknowledgments
This work was performed at the University of California Irvine under grant 3280 from the Gordon and Betty Moore Foundation, funds from UC Irvine, and NASA grant NNX12AB86G; at Caltech's Jet Propulsion Laboratory, Pasadena under a contract with NASA. D.M.H. and D.H. acknowledge support from the NSF Office of Polar ProgramARC-1304137, and the NYU Abu Dhabi Center for Global Sea Level Change grant G1204. Denis Voytenko is thanked for assisting with the preparation for the XCTD bathymetric data file. A 100 m geotiff file is available at ess.uci.edu/group/erignot/node/1535.

References

Argyle, M., S. Ferguson, L. Sander, and S. Sander (2000), AIRGrav results: A comparison of airborne gravity data with GSC test site data, *Leading Edge*, *19*, 1134–1138.
Bamber, J. L., et al. (2013), A new bed elevation dataset for Greenland, *Cryosphere*, *7*, 499–510.
Clarke, T. S., and K. Echelmeyer (1996), Seismic-reflection evidence for a deep subglacial trough beneath Jakobshavns Isbræ, West Greenland, *J. Glaciol.*, *43*(141), 219–232.
Cochran, J. R., and R. E. Bell (2010), *IceBridge Sander AIRGrav L1B Geolocated Free Air Gravity Anomalies, Version 1*, NASA Natl. Snow and Ice Data Cent. Distrib. Act. Arch. Cent., Boulder, Colo.
Echelmeyer, K., T. S. Clarke, and W. D. Harrison (1991), Surficial glaciology of Jakobshavns Isbræ, West Greenland: Part I. Surface morphology, *J. Glaciol.*, *37*(127), 368–382.
Gogineni, P. S., et al. (2014), Bed topography of Jakobshavn Isbræ, Greenland, and Byrd Glacier, Antarctica, *J. Glaciol.*, *60*(223), 813–833.
Holland, D. M., R. H. Thomas, B. de Young, M. H. Ribergaard, and B. Lyberth (2008), Acceleration of Jakobshavn Isbræ triggered by warm subsurface ocean waters, *Nat. Geosci.*, *1*(10), 659–664.
Howat, I. M., A. Negrete, and B. E. Smith (2014), The Greenland Ice Mapping Project (GIMP) land classification and surface elevation datasets, *Cryosphere*, *8*, 1509–1518.
Howat, I. M., A. Yushin, I. Joughin, M. R. van den Broeke, J. T. M. Lenaerts, and B. E. Smith (2011), Mass balance of Greenland's three largest outlet glaciers, 2000–2010, *Geophys. Res. Lett.*, *38*, L12501, doi:10.1029/2011GL047565.
Jakobsson, M., et al. (2012), The International Bathymetric Chart of the Arctic Ocean (IBCAO) version 3.0, *Geophys. Res. Lett.*, *39*, L12609, doi:10.1029/2012GL052219.
Joughin, I., W. Abdalati, and M. A. Fahnestock (2004), Large fluctuations in speed on Greenland's Jakobshavn Isbræ glacier, *Nature*, *432*(7017), 608–610.
Joughin, I., I. M. Howat, M. Fahnestock, B. E. Smith, W. Krabill, R. B. Alley, H. Stern, and M. Truffer (2008), Continued evolution of Jakobshavn Isbræ flowing its rapid speedup, *J. Geophys. Res.*, *113*, F04006, doi:10.1029/2008JF001023.
Joughin, I., B. E. Smith, I. M. Howat, D. Floricioiu, R. B. Alley, M. Truffer, and M. Fahnestock (2012), Seasonal to decadal scale variations in the surface velocity of Jakobshavn Isbrae, Greenland: Observation and model-based analysis, *J. Geophys. Res.*, *117*, F02030, doi:10.1029/2011JF002110.
Joughin, I., B. E. Smith, D. E. Shean, and D. Floricioiu (2014), Brief communication: Further summer speedup of Jakobshavn Isbræ, *Cryosphere*, *8*, 209–214.
Luckman, A., and T. Murray (2005), Seasonal variation in velocity before retreat of Jakobshavn Isbræ, Greenland, *Geophys. Res. Lett.*, *32*, L022519, doi:10.1029/2005GL022519.
Leuschen, C., S. P. Gogineni, F. Rodriguez-Morales, J. Paden, and C. Allen (2010), *IceBridge MCoRDS L2 Ice Thickness*, Natl. Snow and Ice Data Cent., Boulder, Colo.
Morlighem, M., E. Rignot, J. Mouginot, H. Seroussi, and E. Larour (2014), Deeply incised submarine glacial valleys beneath the Greenland ice sheet, *Nat. Geosci.*, *7*, 418–422.
Motyka, R. J., M. Truffer, M. Fahnestock, J. Mortensen, S. Rysgaard, and I. Howat (2011), Submarine melting of the 1985 Jakobshavn Isbræ floating tongue and the triggering of the current retreat, *J. Geophys. Res.*, *116*, F01007, doi:10.1029/2009JF001632.
Parker, R. L. (1973), The rapid calculation of potential anomalies, *Geophys. J. Int.*, *31*, 447–455.
Pedersen, M., W. L. Weng, N. Keulen, and T. Kokfelt (2013), A new seamless digital 1:500 000 scale geological map of Greenland, *Geol. Surv. Den. Greenland Bull.*, *28*, 65–68.
Plummer, J., S. Gogineni, C. van der Veen, C. Leuschen, and J. Li, (2008), Ice thickness and bed map for Jakobshavn Isbræ, *CReSIS Tech. Rep. 2008-1*, Univ. of Kansas, Lawrence, Kans.
Post, A., S. O'Neel, R. J. Motyka, and G. Streveler (2011), A complex relationship between calving glaciers and climate, *Eos Trans. AGU*, *92*(37), 305–306.

Rignot, E., I. Velicogna, M. van den Broeke, and A. Monaghan (2011a), Acceleration of the contribution of the Greenland and Antarctic ice sheets to sea level rise, *Geophys. Res. Lett.*, *38*, L05503, doi:10.1029/2011GL046583.

Rignot, E., J. Mouginot, and B. Scheuchl (2011b), Antarctic grounding line mapping from differential satellite radar interferometry, *Geophys. Res. Lett.*, *38*, L10504, doi:10.1029/2011GL047109.

Rignot, E., J. Mouginot, M. Morlighem, H. Seroussi, and B. Scheuchl (2014), Widespread, rapid grounding line retreat of Pine Island, Thwaites, Smith, and Kohler glaciers, West Antarctica, from 1992 to 2011, *Geophys. Res. Lett.*, *41*, 3502–3509, doi:10.1002/2014GL060140.

Rosenau, R., E. Schwalbe, H.-G. Maas, M. Baessler, and R. Dietrich (2013), Grounding line migration and high-resolution calving dynamics of Jakobshavn Isbræ, West Greenland, *J. Geophys. Res. Earth Surf.*, *118*, 382–395, doi:10.1029/2012JF002515.

Schoof, C. (2007), Ice sheet grounding line dynamics: Steady states, stability, and hysteresis, *J. Geophys. Res.*, *118*, F03S28, doi:10.1029/2006JF000664.

Sergienko, O. V., T. T. Creyts, and R. C. A. Hindmarsh (2014), Similarity of organized patterns in driving and basal stresses of Antarctic and Greenland ice sheets beneath extensive areas of basal sliding, *Geophys. Res. Lett.*, *41*, 3925–3932, doi:10.1002/2014GL059976.

Shapero, D. R., I. R. Joughin, K. Poinar, M. Morlighem, and F. Gillet-Chaulet (2016), Basal resistance for three of the largest Greenland outlet glaciers, *Geophys. Res. Earth. Surf.*, *121*, 168–180, doi:10.1002/2015JF003643.

Studinger, M., R. E. Bell, and N. Frearson (2008), Comparison of AIRGrav and GT-1A airborne gravimeters for research application, *Geophysics*, *73*(6), 151–161.

Thomas, R. (2004), Force-perturbation analysis of recent thinning and acceleration of Jakobshavn Isbrae, Greenland, *J. Glaciol.*, *50*(168), 57–66.

Thomas, R., W. Krabill, E. Frederick, and K. Jezek (1995), Thickening of Jacobshavns Isbræ, West Greenland, measured by airborne laser altimetry, *Ann. Glaciol.*, *21*, 259–262.

Thomas, R., W. Abdalati, E. Frederick, W. B. Krabill, S. Manizade, and K. Steffen (2003), Investigation of surface melting and dynamic thinning on Jakobshavn Isbræ, Greenland, *J. Glaciol.*, *49*(165), 231–239.

Thomas, R., E. Frederick, W. Kravill, S. Manizade, and C. Martin (2009), Recent changes on Greenland outlet glaciers, *J. Glaciol.*, *55*(189), 147–162.

Weidick, A., N. Mikkelsen, C. Mayer, and S. Podlech (2004), Jakobshavn Isbræ, West Greenland: The 2002–2003 collapse and nomination for the UNESCO World Heritage List, *Geol. Surv. Den. Greenland Bull.*, *4*, 85–88.